

EXPANDED METHODS

All studies were performed in compliance with the NIH Guide for the Care and Use of Laboratory Animals (DHHS publication No. [NIH] 85-23, revised 1996). The University of Alabama at Birmingham Institutional Animal Care and Use Committee gave local approval for these studies. The total of 120 mice were used.

Mouse models and surgical protocol. Male C57BL/6J mice 10-12 weeks of age (Jackson Laboratories, stock #000664) were used. To induce pathological LV remodeling and HF, the mice underwent left thoracotomy and left coronary artery ligation (n=19) as previously described.¹⁻³ Sham operated mice (n=12) were used as controls. Anesthesia was induced in mice with tribromoethanol (0.25 mg/g IP). Mice were then intubated and ventilated with a MiniVent Mouse Ventilator (Type 845, Harvard Apparatus) at 125-150 breaths/minute, with anesthesia maintained using 1-2% isoflurane and body temperature kept at 37°C using heat lamps and heating pads. Using sterile technique, mice were subjected to a thoracotomy in the 4th intercostal space. With the aid of a dissecting microscope, the proximal left coronary artery was visualized and permanently occluded with 8.0-prolene suture, 1 mm distal to the left atrial appendage border. Successful occlusion was confirmed by the production of pallor and dyskinesia in the distal myocardium. In sham animals, the suture was passed but not tied. The chest was then closed in layers using 5.0 silk and the mice were weaned off isoflurane anesthesia. Upon recovery of spontaneous respiration, the intubation tube was removed and the mice were recovered in a temperature-controlled area supplemented with 100% oxygen. The mice were then followed for 8 weeks after operation and evaluated for the various readouts.

Echocardiography. Mouse echocardiography was performed under anesthesia with tribromoethanol (0.25 mg/g IP), and light (~1%) isoflurane as needed, using a VisualSonics Vevo 770 High-Resolution System with a RMV707B scanhead. Mice were imaged on a heated, bench-mounted adjustable rail system (Vevo Imaging Station) that allowed steerable and hands-free manipulation of the ultrasound transducer. Two echocardiographers performed the

studies and were blinded as to the specific experimental group. Left ventricular (LV) end-diastolic and end-systolic volumes (EDV and ESV) were planimeted from the long-axis images using the modified Simpson's method. LV systolic function was indexed by single plane LV ejection fraction ($EF = [EDV-ESV]/EDV$).

Isolation of splenocytes. Eight weeks after coronary ligation or sham operation, the spleen was removed aseptically and placed in a 35 mm tissue culture dish with ~5 mL of DMEM culture medium (Gibco, Invitrogen). Splenocytes were isolated according to the protocol of Lavelle et al,⁴ with slight modifications. Briefly, the spleen was finely minced using a scalpel. Repeated pipetting was used to disperse cells from minced fragments, and single cells were transferred to a fresh tube and kept on ice. For larger tissue pieces, the procedure was repeated several times in the dish with fresh DMEM. The final cell suspension was pipetted through a nylon cell strainer, 100 μ m (BD Falcon), into a fresh tube and centrifuged at 150g for 5 min at 4°C. The supernatant was decanted, and the pellet re-suspended in 0.4 ml of RBC lysis buffer (eBiosciences) for 5 min at room temperature (RT). The addition of fresh DMEM neutralized the erythrocyte lysis. Pelleted splenocytes were then re-suspended in fresh DMEM (0.5-1.0 mL).

Isolation of bone marrow (BM) and peripheral blood cells. After mice were sacrificed, femurs and tibiae were dissected from the adherent soft tissue. The tip of each bone was removed with scissors, and the marrow was flushed with DMEM using a 27-gauge needle and aspirated. BM cells were filtered through a 100 μ m nylon cell strainer (BD Falcon), sedimented at 150g for 5 min at 4°C, and re-suspended in RBC lysis buffer. After complete erythrocyte lysis, BM cells were re-suspended in fresh 1-2 mL DMEM.

Peripheral blood (~500 μ L) was collected in BD Microtainer tubes with EDTA. Erythrocytes were lysed with 2 mL RBC lysis buffer for 5 min on ice. Leukocytes were collected by centrifugation (380g for 10 min at 4°C), and resuspended in 400 μ L of ice-cold flow cytometry staining buffer (eBioscience).

Isolation of mononuclear cells from the heart. Single mononuclear cells were isolated from sham and failing hearts following the method of Austyn et al.⁵ Mouse hearts were excised *in toto* and placed in heparinized saline. After removal of epicardial fatty tissue and the aorta, the heart was finely minced into ~1-2 mm pieces and blood was removed by repeated washing in saline (with stepwise reductions in added heparin). The tissue was digested with collagenase (Worthington, 1mg/ml), trypsin (Gibco, Invitrogen, 0.1%), and DNase (5 Prime, 10 µg/ml) in 10 mL RPMI media (Gibco) for 45 min at 37°C with occasional shaking. Released cells were separated from solid tissue by filtering through a 100 µm nylon cell strainer (BD Falcon), washed with R10 media (RPMI-1640 supplemented with 10% heat-inactivated FCS, 2mM-L-Glutamine, 25 µM-2-Mercaptoethanol, 1% penicillin/streptomycin), and placed on ice. These steps were repeated 2-3 times to digest the remaining tissue. Any residual solid tissue was treated sequentially with EDTA (2 mM) in digestion media for 10 min at 37°C, collagenase (2 mg/ml) in R10 media for 20 min at 37°C, and released cells filtered through the strainer. All collected cells were pooled and pelleted at 150g for 5 min at 4°C. Single cell suspensions were layered on Ficoll gradient solution and centrifuged at 2000g for 20 min. To reduce myocyte contamination in the mononuclear cell suspension, 75% of the total volume (excepting cell debris) was collected and washed in R10 media. The presence of nucleated cells was confirmed by DAPI staining during flow cytometry analysis. In a separate aliquot, cell viability (>80%) was confirmed using the trypan blue exclusion method.

Flow Cytometry. Isolated cell suspensions were incubated for 30 min at RT in a cocktail of fluorophore-labeled mAbs (BD Biosciences or as otherwise indicated), as appropriate for the specific study, against: F4/80-Pacific Blue; CD8-FITC; CD45R/B220-APC; CD11b-605-NC (eBiosciences); Gr-1-APC (eBiosciences); CD11c-PE-Cy7; CD86-PE-Cy5; CD206-FITC; Siglec-H-efluor 660 (eBiosciences), CD45.1-FITC (Miltenyi Biotech); CD45.2-PE. Lineage (Lin)1 antibody cocktail was used for DC identification (to exclude thymocytes: CD90.2-PE, natural killer cells: NK1.1-PE, CD49B-PE, and granulocytes: Gr-1-PE), and Lin2 antibody cocktail was

used for macrophage/monocyte subset identification (CD90.2-PE, NK1.1-PE, CD49B-PE, and CD45R/B220-PE for B-cells). In separate assessments of splenic T-cells, cell suspensions were incubated with CD3-FITC, CD4-650 NC and CD8-605 NC (eBiosciences). Of note, the anti-Gr-1 antibody recognizes both Ly6C and Ly6G antigens.⁶

Activated macrophages/monocytes were identified as CD11b⁺F4/80⁺ cells.^{7, 8} Pro-inflammatory monocytes were identified as Lin2⁻CD11b⁺F4/80⁺Gr-1^{hi} and anti-inflammatory monocytes as Lin2⁻CD11b⁺F4/80⁺Gr-1^{low} cells.⁷⁻¹⁰ Pro-inflammatory M1 and anti-inflammatory M2 macrophages in tissue were sub-classified from Lin2⁻CD11b⁺F4/80⁺ cells based on the absence or presence of CD206 (mannose receptor) expression.¹¹ Dendritic cells were identified as Lin1⁻CD11c⁺ cells.^{9, 10, 12} Classical dendritic cells (cDC) were identified as Lin1⁻CD11c⁺B220⁻, whereas non-classical plasmacytoid dendritic cells (pDC) were identified as Lin1⁻CD11c^{+/low}B220⁺.^{10, 12-14} In some studies, pDCs were identified as Siglec-H⁺ cells.¹⁵ Lymphoid cDCs were further subdivided as CD8⁺ or CD8⁻,^{10, 12} and pDCs as CD86⁺ or CD86⁻ (classical costimulatory molecule and marker of pDC maturity).¹⁶ Helper and cytotoxic T-cells were characterized as CD3⁺CD4⁺ and CD3⁺CD8⁺CD4⁻ cells, respectively.¹⁷ For the heart, spleen, and BM, identified cells were normalized for total cell population. For peripheral blood, cell numbers were normalized for the total lymphocyte and monocyte gate. Data were acquired on an LSRII flow cytometer (BD Biosciences) and analyzed with FlowJo software, version 7.6.3.

Immunohistochemistry and confocal microscopy. Formalin-fixed, paraffin-embedded hearts and spleens from sham and HF mice were sectioned at 5 μm thickness, deparaffinized and rehydrated; (immuno)histological staining was performed as previously described.^{1, 3} Masson's trichrome was used to evaluate tissue fibrosis and general histology (heart and spleen), and Alexa Fluor 488-conjugated wheat-germ agglutinin (WGA; Invitrogen) for myocyte area.

Myocardial apoptosis was evaluated using the DeadEnd Fluorometric TUNEL System (Promega) as previously described.^{3, 18} This assay kit catalytically incorporates fluorescein-12-

dUTP at the 3'-ends of fragmented DNA in apoptotic cells using recombinant terminal deoxynucleotidyl transferase (rTdT). Deparaffinized and rehydrated tissue sections were treated with Proteinase K (20 µg/ml) for 15 min at 37°C and then fixed with 4% methanol-free formaldehyde solution in PBS. All subsequent steps were performed following the manufacturer's instructions. Cardiomyocytes were identified by staining with anti-troponin I antibody (Santa Cruz Biotechnology) followed by Alexa Fluor 555-conjugated secondary antibody (Invitrogen) using the protocol below, and sections were counterstained with 4',6-diamidino-2-phenylindole (DAPI, Invitrogen) to label nuclei blue. TUNEL-positive nuclei (cyan staining) were visualized directly by confocal microscopy (Zeiss LSM710) with nuclear staining confirmed using z-axis sections. Images were taken with a 63x objective lens at five different locations in each tissue section. DNase (10 U/ml)-treated sections were used as positive controls. Sections without rTdT treatment were used as negative controls.

For immunostaining, deparaffinized and rehydrated sections were incubated for 20 min with 10 mmol/L citric acid (pH 6.0) and then treated with enzymatic antigen retrieval to recover antigenicity. Nonspecific binding was blocked with 5% normal goat serum and 0.05% saponin (Sigma) in PBS (pH 7.4) for 30 min. Sections were blocked and then incubated with the appropriate primary antibody in PBS with 1% BSA and 0.05% saponin for 1 h at 37°C against: CD11b/ITAM (Epitomics), CD11c (eBiosciences), F4/80 (eBiosciences), CD169 (R&D Systems), high mobility group box-1 (HMGB1, IBL International), and CD45.2-PE (BD Biosciences). Tissue sections were then incubated for 30 min at room temperature with respective secondary antibodies conjugated with Alexa 488, 555, or 647 (Invitrogen), and counterstained with DAPI to label nuclei. Images were made with a 63x objective lens at five different locations in each tissue section. Mean fluorescence intensity was evaluated using imageJ 1.47V software for at least five images/heart.

Myocyte area and cardiac fibrosis were quantified from 5-6 high-power fields per section in the remote non-infarcted area of the heart using Image J and Metamorph software,

respectively. In the spleen, CD11b positive cells in the subcapsular red pulp were counted in 3-5 high power fields per section. Data for each group were calculated from 12-15 sections and 4-5 mice from each group. The measurements and calculations were conducted in a blinded manner. Confocal microscopy was carried out on an LSM710 microscope (Zeiss) and Z-stack images were acquired according to standard protocols.

Cytometric bead array (CBA) immunoassay for serum cytokines. Peripheral blood was allowed to clot at RT for 2 h. After centrifugation at 2,000 rpm for 10 min, serum was collected and stored at -20°C until assays were performed. Serum concentrations of TNF, monocyte chemoattractant protein (MCP)-1, interferon (IFN)- γ , interleukin (IL)-6, IL-10, and IL-12p70 were measured simultaneously using a CBA Mouse Inflammation Kit (BD Biosciences). Briefly, 50 μL of chemokine capture bead mixture was incubated with 50 μL of either recombinant standard or sample and 50 μL of PE-conjugated detection antibody for 2 h at RT. The mixture was washed to remove unbound PE detection reagent before data acquisition on a BD LSRII flow cytometer. Analysis was performed using FCAP Array software.

Splenocyte gene expression by quantitative real-time PCR. Mononuclear splenocytes were cultured in serum free DMEM media for 24 h after isolation ($2-3 \times 10^6$ cells/well). The cells were then collected and stored at -80°C in TRIzol reagent (Invitrogen) for subsequent RNA isolation. Total RNA levels were quantified and sample purity assessed using the ratio of absorbance at 260 and 280 nm by NanoDrop 1000 Spectrophotometer (Thermo Scientific). Subsequent cDNA synthesis and quantitative real-time PCR using SYBR Green (Life Technologies) were performed as described previously.^{1, 2, 18} Briefly, total RNA (500 ng) was reversed transcribed using High Efficiency cDNA Synthesis Kit (Life Technologies). Relative levels of mRNA transcripts for TNF, IL-1 β , IL-2, IL-4, IL-5, IL-6, IL-10, IL-13, IFN- γ , inducible nitric oxide synthase (iNOS), C-C chemokine receptor type 2 (CCR2), CCR5, chemokine (C-C motif) ligand 5 (CCL5), chemokine (C-X-C motif) receptor 3 (CXCR3), CX3C chemokine receptor 1 (CX3CR1), toll-like receptor (TLR)1, TLR7, TLR9, TLR12, transforming growth factor

(TGF)- β , HMGB1, S100A8, S100A9, and galectin-3 were determined using forward and reverse primer pairs detailed in Supplemental Table I, and normalized to 18s rRNA expression using the $\Delta\Delta C_T$ comparative method.¹

Survival splenectomy and splenocyte adoptive transfer. In a separate sub-group, male (CD 45.2) C57BL/6J mice (n = 36) underwent coronary ligation or sham operation. Eight weeks later, survival splenectomy (or, in some mice, sham abdominal surgery) was performed using standard surgical techniques.¹⁹ Briefly, mice were anesthetized with tribromoethanol (0.25 mg/g IP) and anesthesia was maintained with 1% isoflurane as needed. After sterilizing the surgical area, a ~1 cm incision was made in the left subcostal region, and the peritoneum was opened to exteriorize the spleen. The spleen was retracted away from the pancreatic tail, the splenic bundle was ligated at the hilum using 8.0 prolene ligature, and then the spleen was removed intact. For sham operations, the splenic bundle and spleen were left intact. The procedure required ~10–15 minutes to complete; totality of splenectomy was ensured by close examination at the time of operation and confirmed during postmortem examination. Splenocytes from sham-operated and HF mice were used for the adoptive transfer studies described below. Splenectomized mice (and sham abdominal surgery controls) were subsequently followed for 8 more weeks with serial echocardiography.

For adoptive transfer studies, splenocytes were prepared as described previously.²⁰ Briefly, single cell suspensions were prepared from spleens isolated from sham-operated (n=8) and HF mice (n=7). The erythrocytes were lysed with RBC lysis buffer (eBioscience, CA). Single cell suspensions were then layered on Ficoll-Paque (GE Healthcare) gradient and centrifuged at 2000g for 20 min to separate mononuclear cells and exclude granulocytes and residual erythrocytes. Mononuclear cells were collected, washed three times with sterile PBS, and resuspended in sterile PBS. Cells were then pooled from either sham or HF mice and resuspended in 5 ml PBS. Mononuclear cells were injected (~17 X 10⁶ cells in 100 μ L PBS per animal via tail vein) into naïve CD 45.1 C57BL/6J mice (7 mice receiving sham splenocytes and

7 mice receiving HF splenocytes).

As an additional control for adoptive transfer, we also isolated splenocytes from CD45.2 C57BL/6J mice (male, 6-8 weeks) treated with either lipopolysaccharide (LPS) to induce systemic inflammation or PBS control. LPS (0.4 mg/kg) or PBS (0.2 mL) was injected i.p. daily for two consecutive days (n = 5 per group). Spleens were aseptically harvested 24 h after the last i.p. dose, and the mononuclear cell population was isolated and injected via tail vein into naïve CD45.1 C57BL/6 recipient mice (n = 7 per group receiving either LPS-splenocytes or PBS-splenocytes) as above.

Statistical Analysis. Continuous data are summarized as mean \pm standard deviation (SD). Statistical comparisons were performed using the unpaired student's t-test when comparing two groups. For comparisons of more than two groups, two-way ANOVA was used with Bonferroni post-test to adjust for multiple comparisons. A p value of < 0.05 was considered statistically significant.

REFERENCES

1. Hamid T, Gu Y, Ortines RV, Bhattacharya C, Wang G, Xuan YT, Prabhu SD. Divergent tumor necrosis factor receptor-related remodeling responses in heart failure: Role of nuclear factor- κ B and inflammatory activation. *Circulation*. 2009;119:1386-1397
2. Hamid T, Guo SZ, Kingery JR, Xiang X, Dawn B, Prabhu SD. Cardiomyocyte NF- κ B p65 promotes adverse remodelling, apoptosis, and endoplasmic reticulum stress in heart failure. *Cardiovasc Res*. 2011;89:129-138
3. Wang G, Hamid T, Keith RJ, Zhou G, Partridge CR, Xiang X, Kingery JR, Lewis RK, Li Q, Rokosh DG, Ford R, Spinale FG, Riggs DW, Srivastava S, Bhatnagar A, Bolli R, Prabhu SD. Cardioprotective and antiapoptotic effects of heme oxygenase-1 in the failing heart. *Circulation*. 2010;121:1912-1925
4. Lavelle GC, Sturman L, Hadlow WJ. Isolation from mouse spleen of cell populations with high specific infectivity for scrapie virus. *Infect Immun*. 1972;5:319-323
5. Austyn JM, Hankins DF, Larsen CP, Morris PJ, Rao AS, Roake JA. Isolation and characterization of dendritic cells from mouse heart and kidney. *J Immunol*. 1994;152:2401-2410
6. Fleming TJ, Fleming ML, Malek TR. Selective expression of Ly-6G on myeloid lineage cells in mouse bone marrow. RB6-8C5 mAb to granulocyte-differentiation antigen (Gr-1) detects members of the Ly-6 family. *J Immunol*. 1993;151:2399-2408

7. Robbins CS, Swirski FK. The multiple roles of monocyte subsets in steady state and inflammation. *Cell Mol Life Sci.* 2010;67:2685-2693
8. Gordon S, Taylor PR. Monocyte and macrophage heterogeneity. *Nat Rev Immunol.* 2005;5:953-964
9. Geissmann F, Manz MG, Jung S, Sieweke MH, Merad M, Ley K. Development of monocytes, macrophages, and dendritic cells. *Science.* 2010;327:656-661
10. Shortman K, Naik SH. Steady-state and inflammatory dendritic-cell development. *Nature reviews. Immunology.* 2007;7:19-30
11. Biswas SK, Mantovani A. Macrophage plasticity and interaction with lymphocyte subsets: Cancer as a paradigm. *Nat Immunol.* 2010;11:889-896
12. Kushwah R, Hu J. Complexity of dendritic cell subsets and their function in the host immune system. *Immunology.* 2011;133:409-419
13. Hadeiba H, Lahl K, Edalati A, Oderup C, Habtezion A, Pachynski R, Nguyen L, Ghodsi A, Adler S, Butcher EC. Plasmacytoid dendritic cells transport peripheral antigens to the thymus to promote central tolerance. *Immunity.* 2012;36:438-450
14. Hochrein H, O'Keefe M, Wagner H. Human and mouse plasmacytoid dendritic cells. *Human Immunol.* 2002;63:1103-1110
15. Blasius AL, Colonna M. Sampling and signaling in plasmacytoid dendritic cells: The potential roles of Siglec-H. *Trends Immunol.* 2006;27:255-260
16. Ito T, Yang M, Wang YH, Lande R, Gregorio J, Perng OA, Qin XF, Liu YJ, Gilliet M. Plasmacytoid dendritic cells prime IL-10-producing T-regulatory cells by inducible costimulator ligand. *J Exp Med.* 2007;204:105-115
17. Kitchen SG, Jones NR, LaForge S, Whitmire JK, Vu BA, Galic Z, Brooks DG, Brown SJ, Kitchen CM, Zack JA. CD4 on CD8+ T cells directly enhances effector function and is a target for HIV infection. *Proc Natl Acad Sci USA.* 2004;101:8727-8732
18. Ismahil MA, Hamid T, Haberzettl P, Gu Y, Chandrasekar B, Srivastava S, Bhatnagar A, Prabhu SD. Chronic oral exposure to the aldehyde pollutant acrolein induces dilated cardiomyopathy. *Am J Physiol Heart Circ Physiol.* 2011;301:H2050-2060
19. Wang HX, Yi SQ, Li J, Terayama H, Naito M, Hirai S, Qu N, Yi N, Itoh M. Effects of splenectomy on spontaneously chronic pancreatitis in aly/aly mice. *Clin Dev Immunol.* 2010;2010:614890
20. Kodama M, Matsumoto Y, Fujiwara M. In vivo lymphocyte-mediated myocardial injuries demonstrated by adoptive transfer of experimental autoimmune myocarditis. *Circulation.* 1992;85:1918-1926

Supplemental Table I. Forward and Reverse Primers for Real-Time PCR

Gene Name	Gene ID	Accession #	Sequence
TNF- α	21296	NM_013693	F: CAGCCGATGGGTTGTACCTT R: GGCAGCCTTGTCCCTTGA
IL-1 β	16176	NM_008361	F: AGTTGACGGACCCCAAAGA R: GGACAGCCCAGGTCAAAGG
IL-2	16183	NM_008366	F: AAATAAAGGGCTCTGACAACACA R: CACCACAGTTGCTGACTCATCA
IL-4	16189	NM_021283	F: GGAGATGGATGTGCCAAACG R: CGAGCTCACTCTCTGTGGTGT
IL-5	16191	NM_010558	F: TGCACCTGAGTGTTCTGACTCTCA R: TGTGCTCATGGGAATCTCCAT
IL-6	16193	NM_031168	F: CCACGGCCTTCCCTACTTC R: TTGGGAGTGGTATCCTCTGTGA
IL-10	16153	NM_010548	F: GATGCCCCAGGCAGAGAA R: CACCCAGGGAATTCAAATGC
IL-13	16163	NM_008355	F: TTGAGGAGCTGAGCAACATCAC R: CCATGCTGCCGTTGCA
IFN- γ	15978	NM_008337	F: TTGGCTTTGCAGCTCTTCT R: TGAAGTGCCGTGGCAGTA
iNOS	18126	NM_010927	F: AGACCTCAACAGAGCCCTCA R: GCAGCCTCTTGTCTTTGACC
CCR2	12772	NM_009915	F: CTGCTCAACTTGGCCATCTCT R: GTGAGCCCAGAATGGTAATGTG
CCR5	12774	NM_009917	F: GTCAAACGCTTTTGCAAACG R: TGAGCTTGCACGATCAGGATT
CCL5	20304	NM_013653	F: TCCAATCTTGCAGTCGTGTTTG R: TCTGGGTTGGCACACACTTG
CXCR3	12766	NM_009910	F: TTGCCCTCCCAGATTTTCATC R: TGGCATTGAGGCGCTGAT
CX3CR1	13051	NM_009987	F: TCGGTCTGGTGGGAAATCTG R: GGCTTCCGGCTGTTGGT
TLR1	21897	NM_001276445	F: GGCTTTGCAGGAACTCAATGTA R: CCCCACACCCAGGAA
TLR7	170743	NM_133211	F: CAGTGAAGTCTGGCCGTTGA R: CAAGCCGTTGTTGGAGAA
TLR9	81897	NM_031178	F: CCTTCGTGGTGTTCGATAAGG R: CACCCGCAGCTCGTTATACA
TLR12	384059	NM_205823	F: CTGCCACTGTGCCAATGC

			R: ATATGTACGTTTTAGTGGACCGCTTA
TGF- β	21803	NM_011577	F: GCAGTGGCTGAACCAAGGA R: AGCAGTGAGCGCTGAATCG
HMGB1	15289	NM_010439	F: CCCCAATGCACCCAAGAG R: GGCGGTA CT CAGAACAGAACAAG
Galectin-3	16854	NM_001145953	F: CACAATCATGGGCACAGTGAA R: TTCCCTCTCCTGAAATCTAGAACAA
S100A8	20201	NM_013650	F: GGCCTTGAGCAACCTCATTG R: AGAGGGCATGGTGATTCCTT
S100A9	20202	NM_009114	F: TCATGGAGGACCTGGACACA R: CAGCATCATACACTCCTCAAAGCT

SUPPLEMENTAL FIGURE LEGENDS

Supplemental Figure I. Long-term pathological cardiac remodeling after coronary ligation. **A**, Representative M-mode echocardiograms (*Left*) and Masson's trichrome-stained short-axis histological sections (*Right*) from sham-operated mice and mice with permanent coronary ligation and heart failure (HF), 8 weeks after operation. Histological images were taken with a 2X objective; scale bar 1 mm. **B**, Higher power histological images of trichrome (left) and Alexa Fluor 488-conjugated wheat-germ agglutinin (WGA) stains of sham and HF heart sections. **C**, quantitative group data for gravimetric, histological, and echocardiographic analyses from sham and HF mice. EDV and ESV, end-diastolic and end-systolic volume; EF, ejection fraction. Fibrosis and myocyte area were determined in myocardium remote from the infarction. N = 5-7/group.

Supplemental Figure II. Serum cytokine levels in sham and HF mice as determined by cytometric bead array immunoassay. IL, interleukin; TNF, tumor necrosis factor; IFN, interferon, MCP, monocyte chemotactic protein. N = 3-4/group.

Supplemental Figure III. Representative flow cytometry scatter plots for SSC versus Siglec-H fluorescence in mononuclear splenocytes from sham and HF mice, expressed as percentage of the total mononuclear cell population, and corresponding group data. An unstained control sample (*Left*) is also shown for comparison. N = 4-5/group.

Supplemental Figure IV. Representative live cell gates and scatter plots from sham and HF spleens identifying CD3⁺CD4⁺ and CD3⁺CD8⁺CD4⁻ cells as a percentage of total live mononuclear cell population, and corresponding group data. N = 4-5/group.

Supplemental Figure V. Quantitative group data for activated monocytes (Lin2⁻CD11b⁺F4/80⁺ cells), classical DCs (Lin1⁻CD11c⁺B220⁻ cells), and plasmacytoid DCs (Lin1⁻CD11c^{+/low}B220⁺ cells) in bone marrow from sham and HF mice. N = 5-6/group.

Supplemental Figure VI. Serum cytokine levels as determined by cytometric bead array immunoassay in mice with HF (16 weeks after coronary ligation) that underwent either

splenectomy (HF without spleen) or sham abdominal surgery (HF with spleen) 8 weeks after ligation. All values normalized to HF with spleen group. TNF, tumor necrosis factor; MCP, monocyte chemotactic protein; IL, interleukin; IFN, interferon. N = 4-6/group.

Supplemental Figure VII. Representative peripheral blood leukocyte flow cytometry scatter plots for recipient CD45.1⁺ versus donor CD45.2⁺ cells (monocyte-lymphocyte gate) two weeks following splenocyte adoptive transfer (AT) demonstrating low levels of residual circulating CD45.2⁺ donor cells (1.56% in this example). An unstained blood sample is shown for comparison.

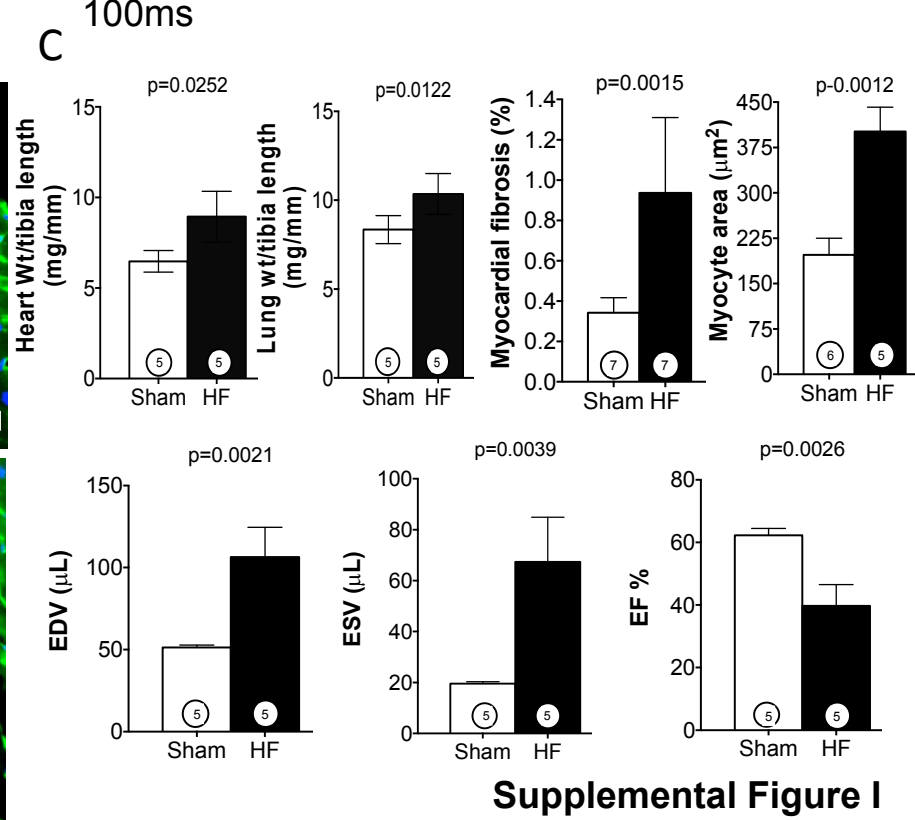
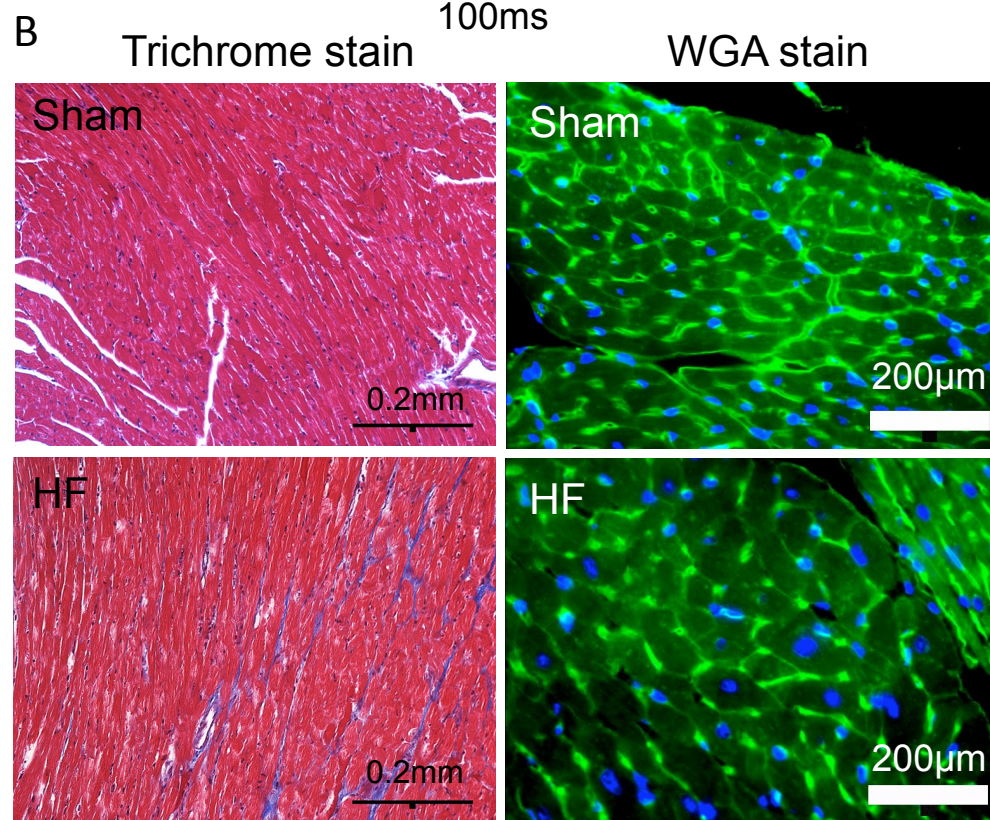
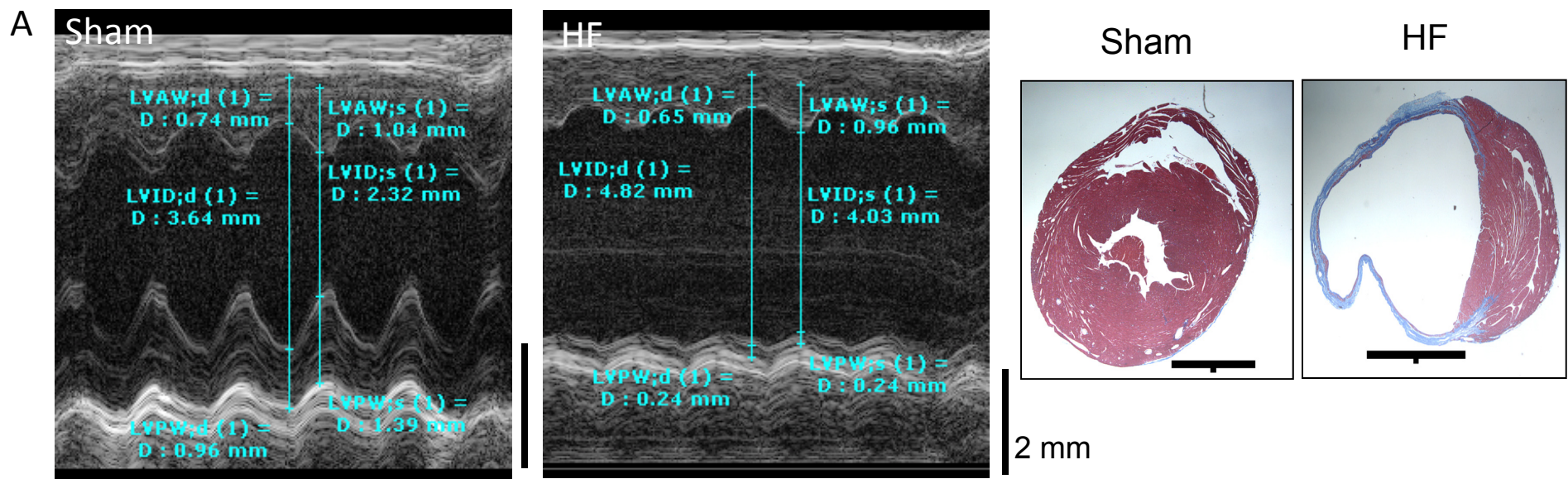
Supplemental Figure VIII. Serum cytokine levels as determined by cytometric bead array immunoassay in mice that received either sham-splenocytes or HF-splenocytes, measured 8 weeks after adoptive transfer. All values normalized to sham-splenocyte group. TNF, tumor necrosis factor; MCP, monocyte chemotactic protein; IL, interleukin; IFN, interferon. N = 3-5/group.

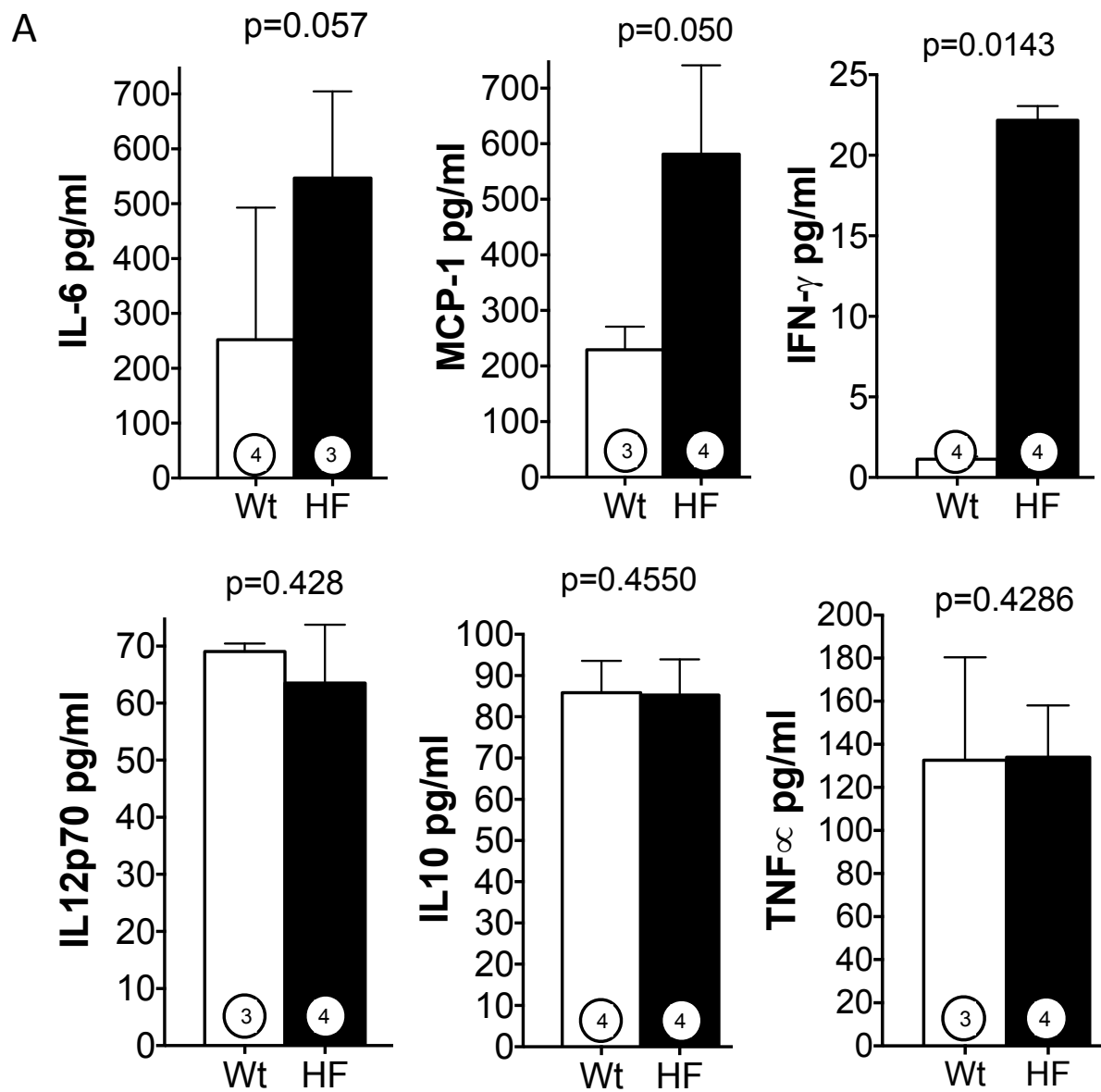
Supplemental Figure IX. A, Lin2⁻CD11b⁺F4/80⁺ circulating monocytes were identified from the monocyte-lymphocyte gate of peripheral blood leukocytes from mice treated with either lipopolysaccharide (LPS) or PBS control for two days. CD11b⁺F4/80⁺ cells were then subdivided as Gr-1 low or high. Representative scatter plots from PBS and LPS treated mice (and unstained sample control) are shown in the top panels and quantitative group data for circulating monocyte subsets in the bottom panels. N = 5/group. **B,** Representative M-mode echocardiograms from recipient mice given mononuclear splenocytes from either PBS- or LPS-treated mice, at baseline (prior to transfer) and 8 weeks after adoptive cell transfer.

Supplemental Figure X. Normalized gene expression of select pro- and anti-inflammatory mediators and TLR pattern-recognition receptors (PRRs) in mononuclear splenocytes isolated from sham-operated and HF mice. *p < 0.05 vs. sham; n = 4-6/group.

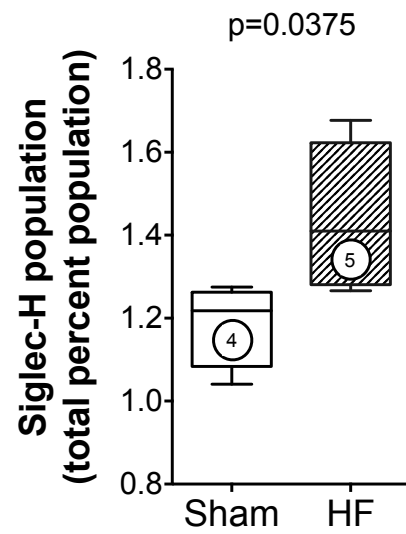
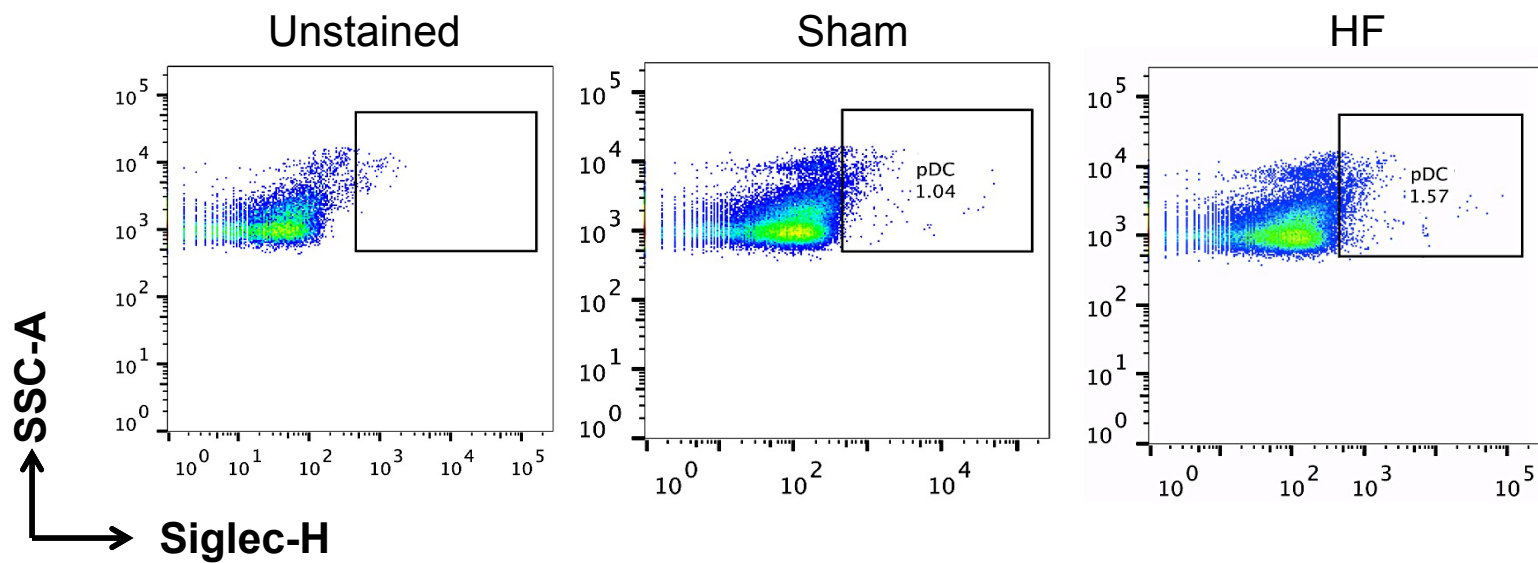
Supplemental Figure XI. A, Representative splenic immunostains for the alarmin HMGB1 from sham-operated and HF mice and corresponding quantitation for HMGB1

fluorescence intensity. WP, white pulp, RP, red pulp, MZ, marginal zone. **B**, Normalized gene expression of the alarmins HMGB1, S100A8, S100A9, and galectin-3 in mononuclear splenocytes isolated from sham and HF mice. n = 4-5/group for **A** and **B**. **C**, Representative confocal images of HMGB1 (green), CD45.2 (red), and DAPI (blue, for nuclei) (immuno)staining of hearts from CD45.1 mice 8 weeks after adoptive transfer of CD45.2 sham- or HF-splenocytes. The yellow arrow indicates a CD45.2⁺HMGB1⁺ cell cluster in the HF-splenocyte recipient heart. The green arrows indicate other areas of HMGB1 expression in recipient myocardium.

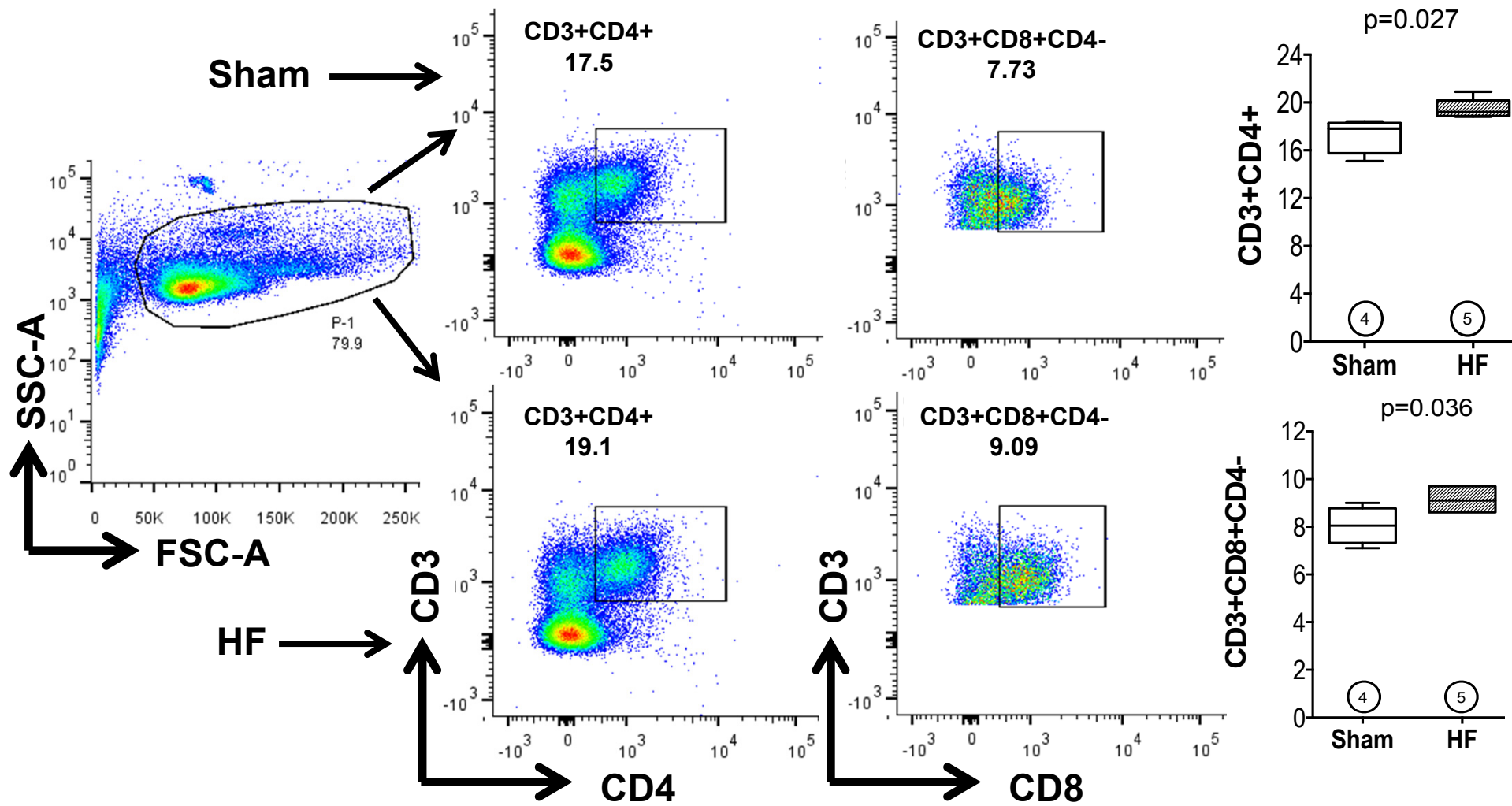




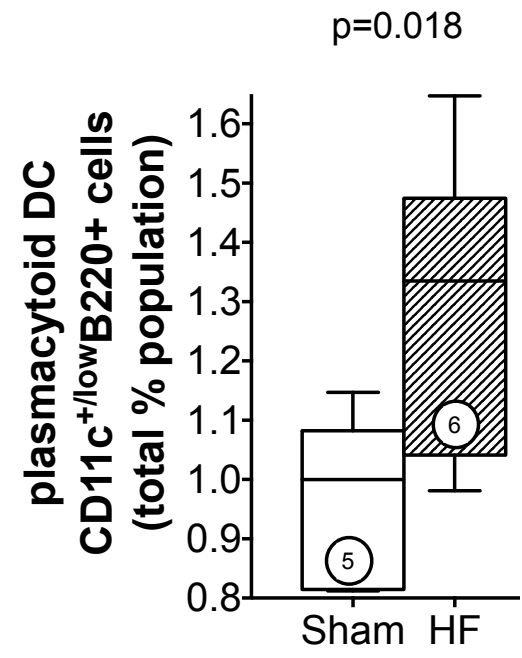
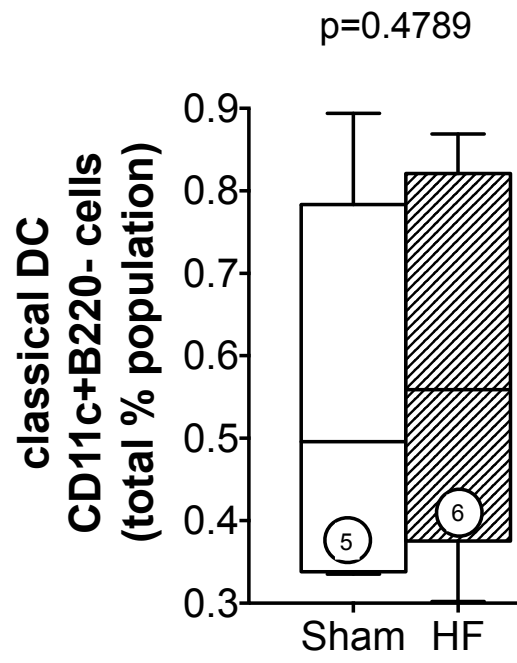
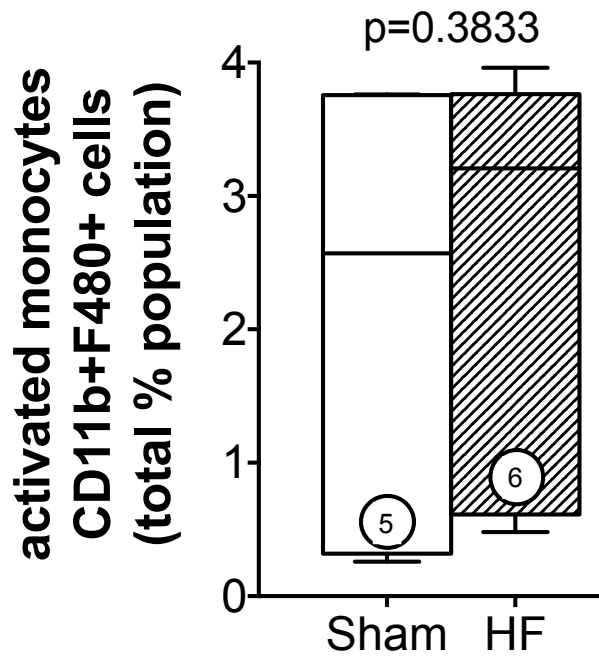
Supplemental Figure II



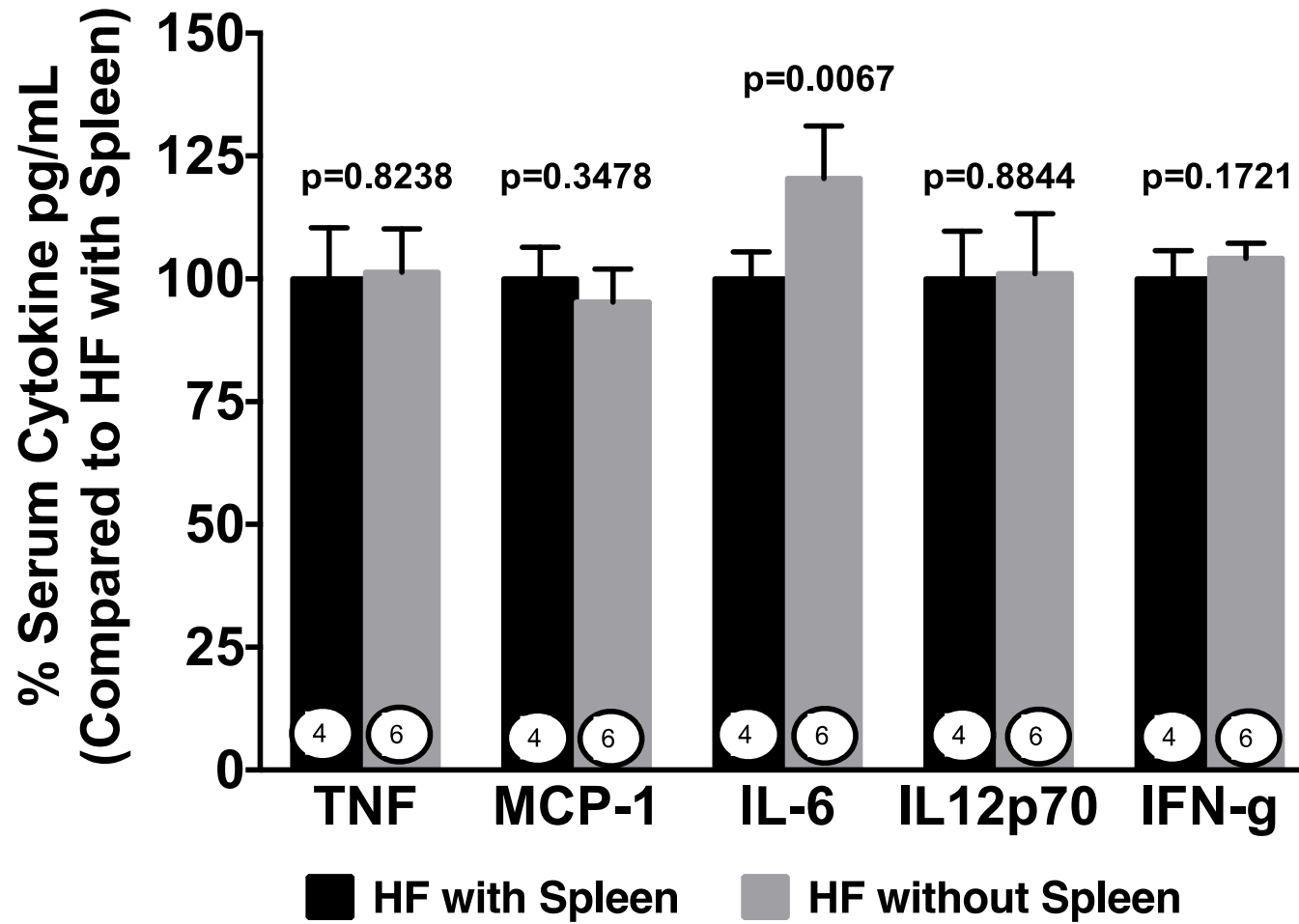
Supplemental Figure III



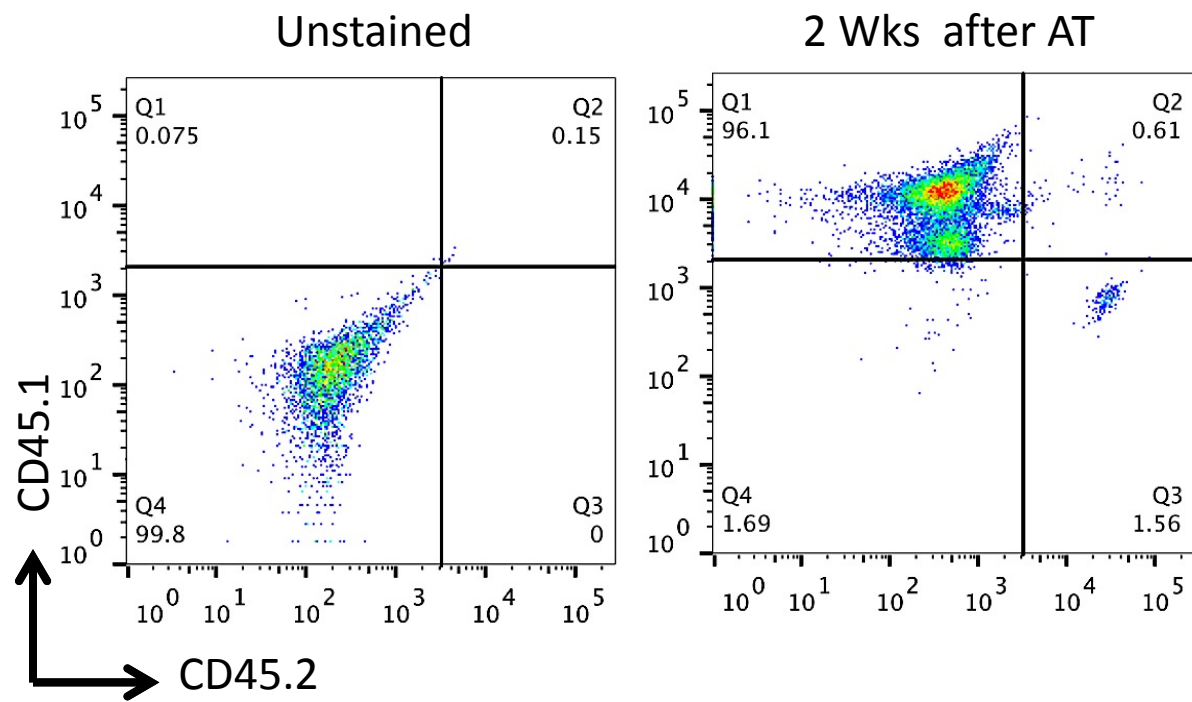
Supplemental Figure IV



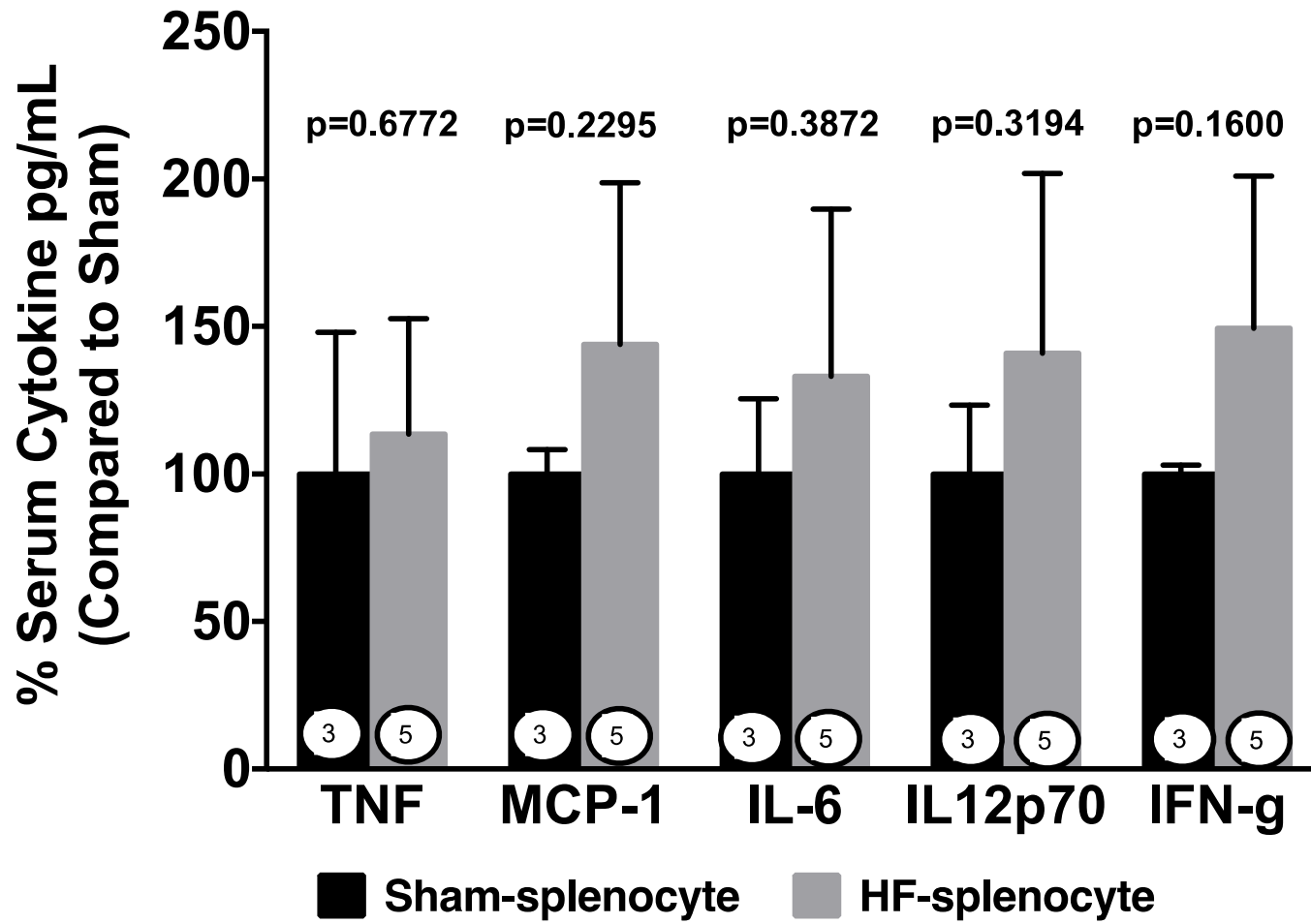
Supplemental Figure V

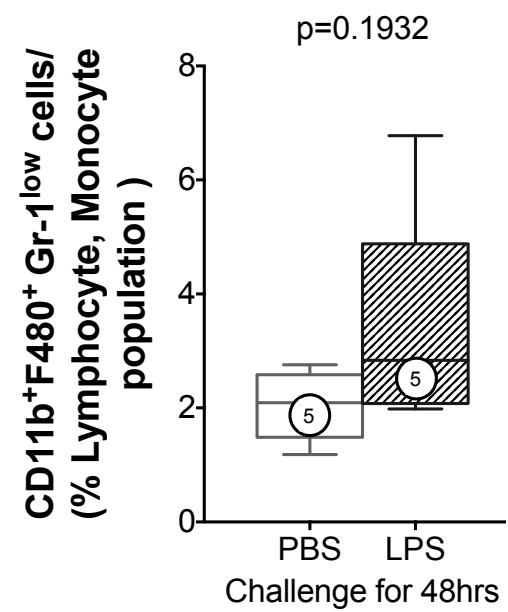
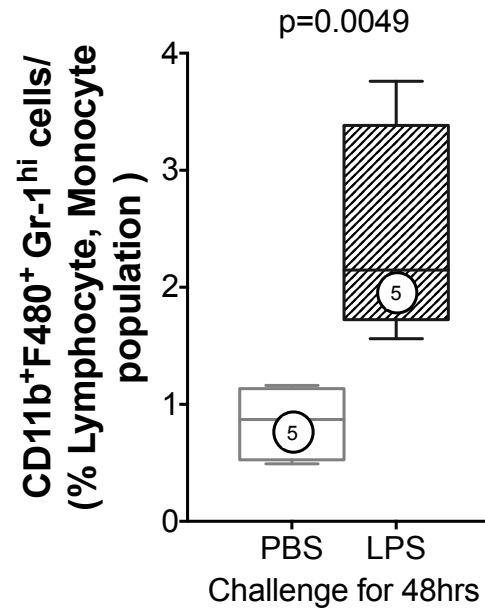
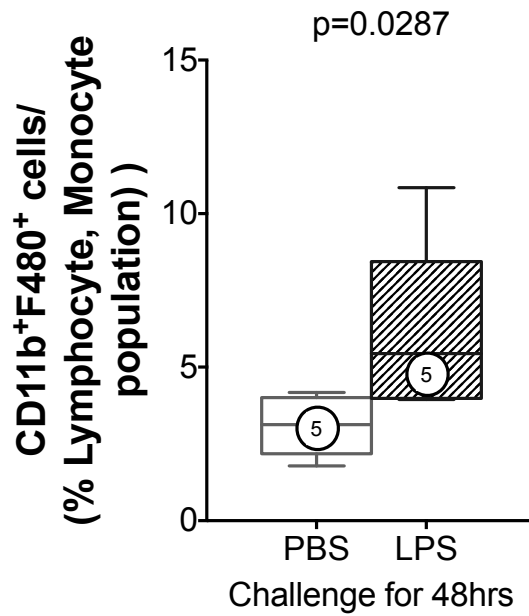
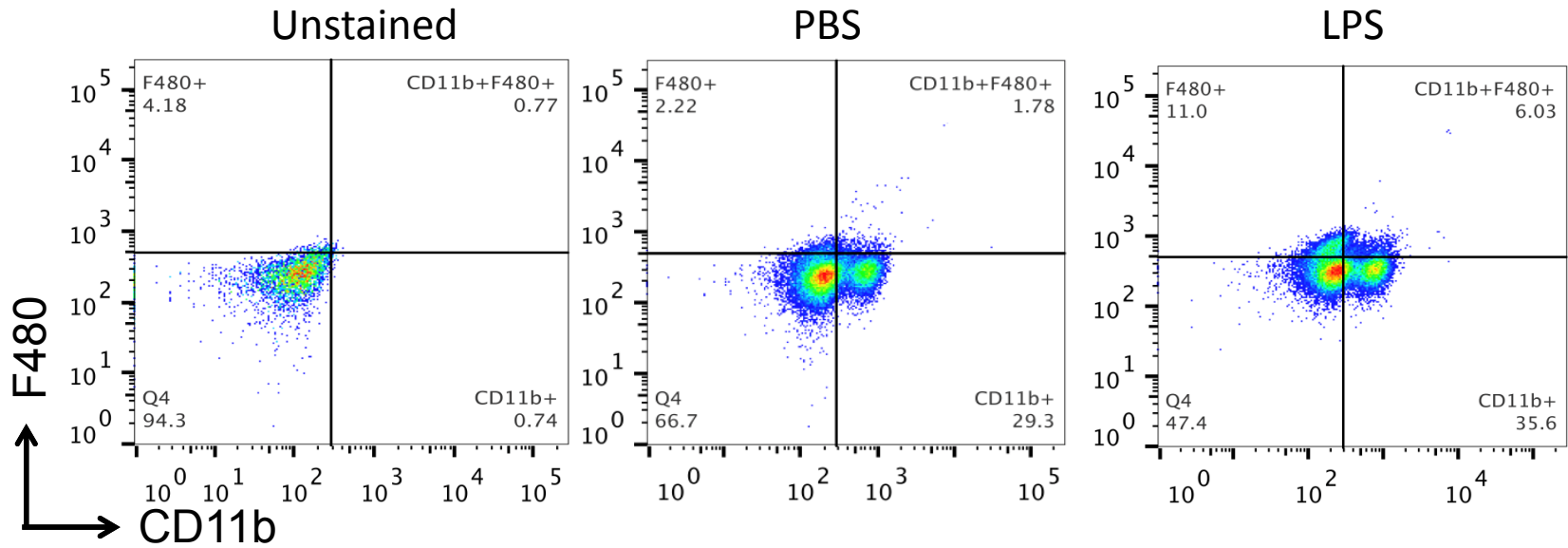


Supplemental Figure VI

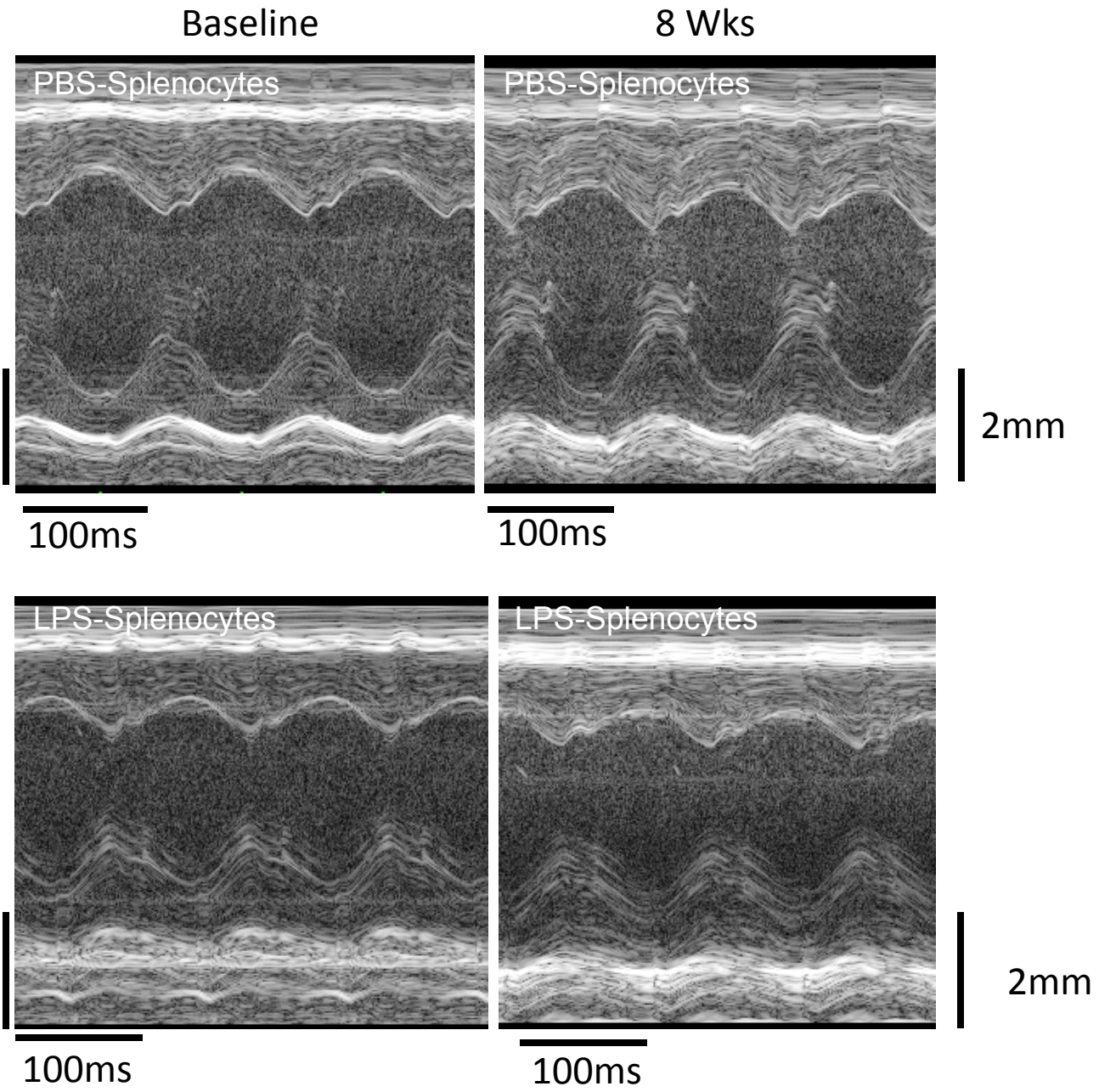


Supplemental Figure VII

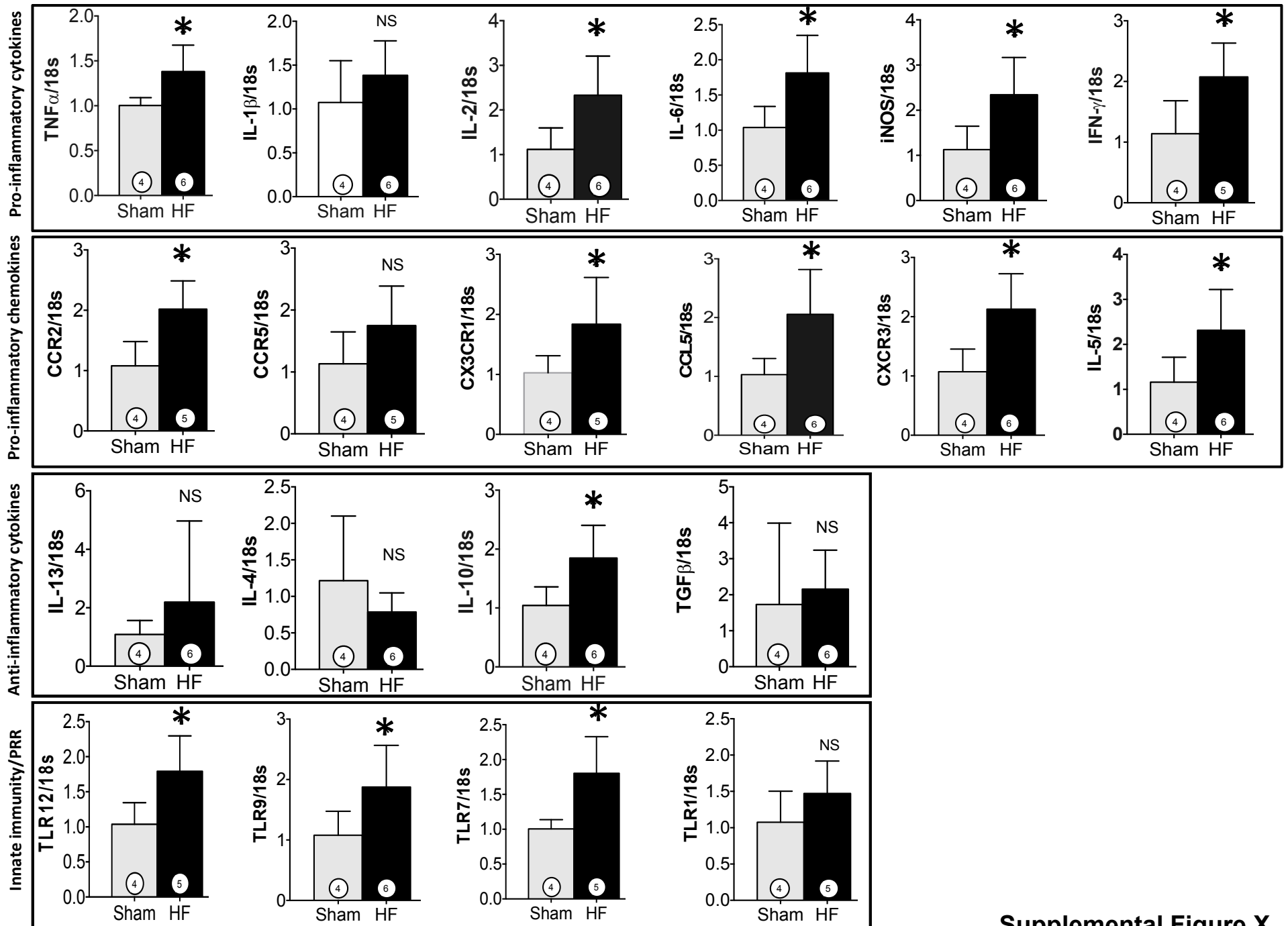




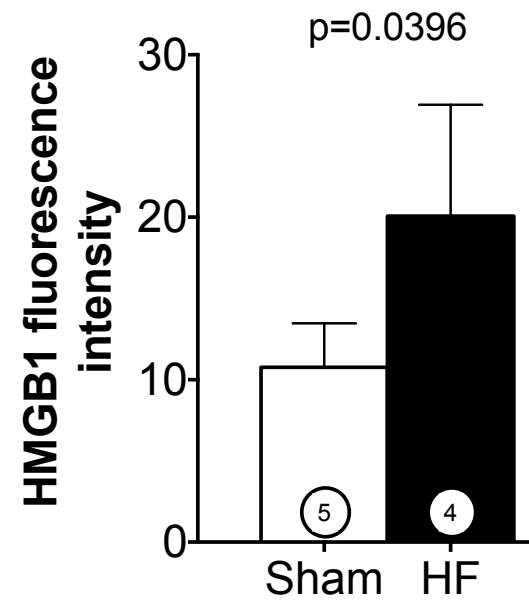
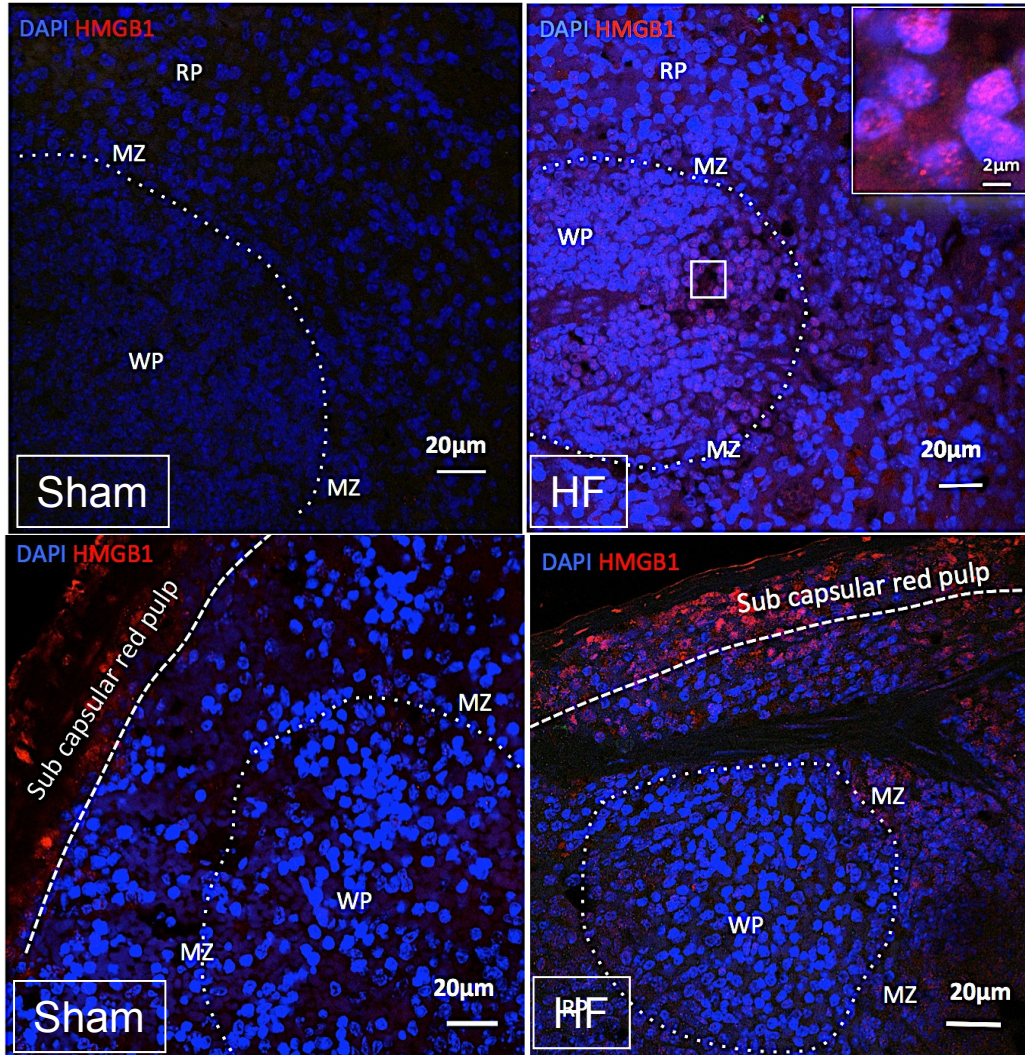
Supplemental Figure IXA



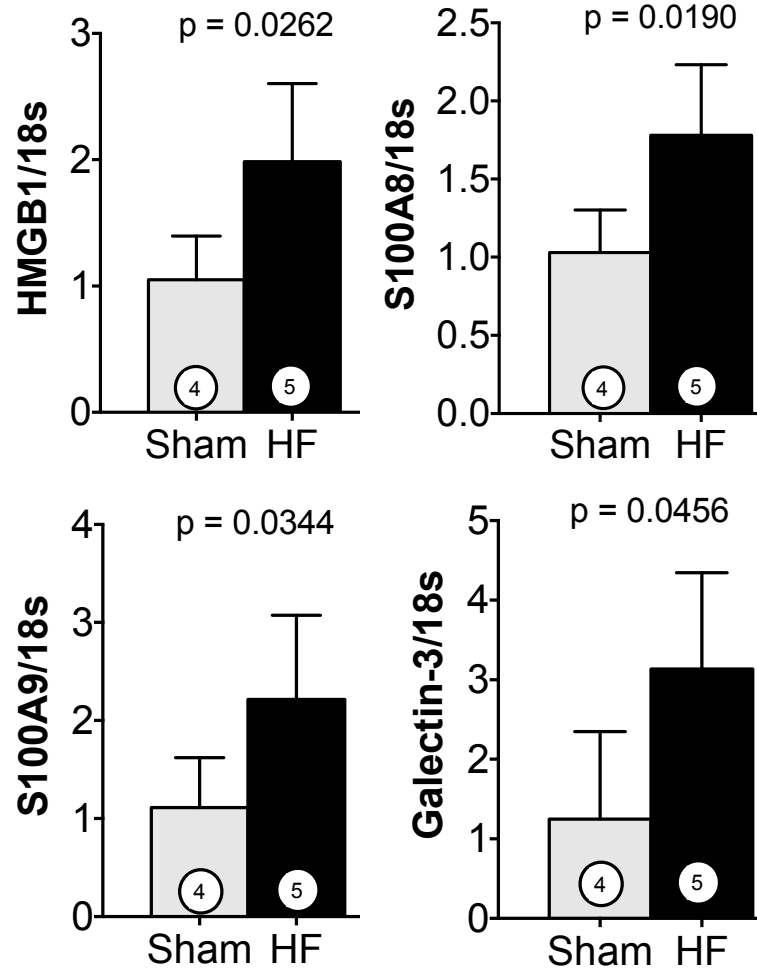
Supplemental Figure IXB



Supplemental Figure X



Supplemental Figure XIA



Supplemental Figure XIB

F

